One Step Sol-Gel Synthesis and Morphostructural Characterization of Sodium Titanate Particles

Florina-Diana Gheorghe[1], *Cristina Rodica* Dumitrescu[1], *Petrache-Ionuț* Gheorghe[1], *György* Deák Habil[1*] and *Sam Sung* Ting[2]

[1]National Institute for Research and Development in Environmental Protection, Bucharest, Romania
[2]Sustainable Environment Research Group (SERG), Centre of Excellence Geopolymer and Green Technology (Cegeogtech), Universiti Malaysia Perlis, Jejawi, 02600 Arau, Perlis, Malaysia

Abstract. Titanate-based materials are attractive inorganic adsorbents for wastewater treatment but also could be used as high performances ceramics. In this study, platelets and wires like morphologies of sodium titanate were successfully synthesized via an unconventional sol-gel method, starting with titanium tetrachloride, $TiCl_4$ and sodium hydroxide, NaOH precursors, and coupled with hydrothermal maturation at 160°C for 24h. Afterwards, through an alkaline hydrothermal maturation, this intermediate phase gradually converted into a sodium titanate with a preserved morphology. The powder thus obtained, was compositionally characterized using X-Ray Diffraction (XRD) and Electron Dispersive Spectroscopy (EDS), structural properties were highlighted by imaging through Scanning Electron Microscopy (SEM) and Thermogravimetric measurements were carried out to determine the transformations that occur between 25-1000 °C. It is shown that a mix of two titanate phase $Na_2Ti_nO_{2n+1}$ with n = 3 and 6 was obtained, having wires and platelet like morphology and micron sizes particles, with a crystallite size of 22 nm grown on Miller indices plane (200). This work was designed to improve the production yield by using an unconventional titanate synthesis method and precursors.

1 Introduction

The rapid development of nanotechnology in recent decades has led to the development of advanced materials with improved properties (i.e. ultrafast responses and strong nonlinearity) that meet the current needs. Among the most studied nanomaterials, sodium titanates have been widely investigated because of their large surface area (up to 478 m^2/g) and pore volume (up to 1.25 cm^3/g) [1], showing great potential in the field of photocatalysis, photoluminescence, ion-exchange systems, photocleavage of water, and solar cells, as well as for biomaterials applications, making thus the technologies more affordable, durable, and environmentally sustainable [2, 3]. The application of sodium titanate in sodium-ion batteries attracts significant attention from researchers worldwide, due to cost-effectiveness and

* Corresponding author: dkrcontrol@yahoo.com

availability as raw materials compared to the lithium-ion counterpart [4]. Sodium titanates have also been used for the removal of heavy metal ions from wastewater [5], as industrialization and urban development releases important quantities of heavy metals into aquatic environments [6, 7]. The present increasing air and water pollution threatens human health as it became an impetuous public concern matter, requiring immediate measures to combat these phenomena [8, 9]. In this respect, alkali titanates offer innovative alternatives for water purifying filters [10], and can also be used as a catalyst in the transesterification process with a 98% conversion rate for biodiesel production [11]. In order to improve the functional properties of the sodium titanates such as photocatalytic activity or ion-exchange and the retention capacity, the grain size and morphology control are required, which can be obtained through a proper synthesis method [8]. Sodium titanate nanostructures showed high abilities to retain radionuclide pollutants that have been released in large amounts by atmospheric nuclear tests, mining and milling of uranium, reprocessing of spent nuclear fuel, and operation, decontamination and decommissioning of nuclear power facilities [12]. New synthesis routes, which can improve the material cost-effectiveness and the functional features development, are always in demand. In this context, the chemical and physical properties of sodium titanates depend on the precursors and the used synthesis method (such as the hydrothermal method, the sol-gel method, the anodizing method and the template synthesis method) [13]. Generally, for the sol-gel method, the sodium salt and titanium salt are used as precursors to form gel, and subsequently, the gel is calcinated to obtain $Na_2Ti_6O_{13}$ [14]. For the hydrothermal method, titanium dioxide (TiO_2) and sodium hydroxide (NaOH) will be stirred in distilled water uniformly, then heated for a long period of time and high temperature, and afterwards the annealing treatment will follow until $Na_2Ti_6O_{13}$ powders are prepared [15]. However, one of the limitations of the hydrothermal method is the long treatment time. To overcome this constraint, sodium chloride (NaCl) flux can be used as a reaction medium, and sodium carbonate (Na_2CO_3) and titanium dioxide (TiO_2) are added into the hot stream to obtain sodium titanate whiskers [13]. Though the flux method reduces the process duration and cost, it still needs a high temperature environment, which is more than 1000 °C [10]. In the interaction of different regents, precursors for Ti and Na, especially using emerging hydrothermal suspension maturation, various morphology of crystalline species were found: rectangular, rhombic, irregular hexagonal, and octagonal, and also acicular and entangled fibrous [16].

Studies show that titanate nanofibers could adsorb heavy metals with a high and irreversible adsorption capacity through ion exchange with cations existing between the layers [17]. If this nanomaterial is used as a filler, it could solve the problems of low adsorption capacity of traditional fillers and secondary pollution caused by desorption [18]. However, the high dispersion of nanomaterials has limited the application of titanate nanofibers as fillers, being thus important to find an appropriate method to best utilize these nanomaterials. Other investigations reported very good results of the fast adsorption processes, completed in ten minutes, using hierarchical hollow sodium titanate microspheres successfully synthesized via a template-assisted method [19]. Silica microspheres were selected as hard templates, a uniformly smooth TiO_2 shell was first deposited onto the surface of the silicon dioxide, SiO_2 cores and after the alkaline hydrothermal process, the silica core was removed and the TiO_2 shell gradually converted into a sodium titanate shell with a preserved morphology [20]. The sodium titanate nanopowder obtained using sol-gel method, starting with titanium isopropoxide, sodium methoxide, Triton X-100, and distillated water, mixed and stirred at room temperature for 24 h, then heated at 82°C for 90 min, also proved the adsorption of selective strontium, Sr pollutants [12, 21].

Good heavy metals adsorption results showed the sodium iron titanates powders $NaFeTiO_4$ and $Na_2Fe_2Ti_6O_{16}$ synthetized by solid state method, using Na_2CO_3, Fe_2O_3 and TiO_2, mixed with a few drops of acetone for 15–20 min and annealed at 900°C for 24 h [21].

Also, sodium titanate with nanotube morphology using hydrothermal synthesis method for 23 h at 160 °C, evidenced a high Brunauer-Emmett-Teller (BET) specific surface and consequently a great adsorption of dyes [15].

Herein, this work proposed to synthesize sodium titanate ($Na_2Ti_nO_{2n+1}$) with n= 3 and 6 using a simple, cheap, and effective one step sol-gel method. For this purpose, NaOH and $TiCl_4$ precursors were used, without the distinct stage of TiO_2 formation. In addition, the proper synthesis route was identified for both platelet and acicular morphology sodium titanate, features gained as a result of hydrothermal maturation. Such structure of sodium titanate powder qualifies the material for the best absorbent properties as water filter against heavy metals and dyes pollutant applications.

2 Materials and methods

2.1 Sodium titanate preparation

All regents and solvents were of analytical grade and used without further purification. Ultra-pure water was used in all experiments. For sol-gel synthesis of sodium titanate, over the 500 mL solution of NaOH 12M (Merck, 99.9%) placed into an ice bath (around 0-5°C), was slowly dripped $TiCl_4$ (Merck) in stoichiometric weight rate Na:Ti = 2:6, under continuous magnetic stirring, for approximately 30 min until a milky white suspension was obtained. This suspension was transferred to a Teflon-lined stainless-steel autoclave with a 1000-mL capacity and heat at 160 °C for 24 h. The maturated titanate suspension was recovered after 7 cycles of washing with distilled water and centrifugation at 5000 rpm for 15 minutes each, until the supernatant pH was constantly around 7, and then the powder was dried at 100 °C for 4 h. The prepared powder was grinded in a porcelain mortar with pestle.

2.2 Compositional and morphostructural characterization methods

The mineralogic phases identification and crystallite size were obtained by X-ray powder diffraction (XRD) using a Bruker D8-Advance X-ray diffractometer with a CuKα radiation source (λ = 1.5418 Å). The 2θ range was between 5–60°. The mass loss of the obtained sodium titanate was obtained through thermogravimetric analysis (TGA) using a NETZSCH STA 449 thermal analyzer. The analysis was performed at a heating rate of 10°C/min under nitrogen. The samples were characterized by using a Hitachi SU-70 scanning electron microscopy (SEM) coupled with energy dispersive spectroscopy (EDS) detector. To enhance the sample conductivity, an AuPd conductive layer was applied by using the SC7620 Mini Sputter Coater/Glow Discharge System.

3 Results and discussion

3.1 Crystalline phase characterisation by X-Ray Diffraction (XRD)

The XRD plot in Fig. 1 shows the result of the XRD investigation on the calcined powder at 600°C in the air atmosphere. Two mineral phases of $Na_2Ti_6O_{13}$ and $Na_2Ti_3O_7$-types sodium titanates were identified in that sample, according to the COD (Compound Open Data) numbers 4000748 and 4000749, respectively.

Corresponding to the sodium titanate diffraction plot, the powder showed good crystallinity, with the most intense diffraction peaks at 2θ values of 11.85°, 14.3°, 24.5°, 29.9°, 30.01°, 30.015°, 30.019°, 33,5°, 43.5° and 48.9°, which correspond to the (200), (101),

(011), (300), (-203), (401), (020) and (006) Miller family planes, respectively. Actually, the sodium titanate type detected at a diffraction angle, 2θ of 11.85°, corresponds to the main (200) crystal plane of the monoclinic structure of $Na_2Ti_6O_{13}$ [19]. Contrary to expectation, the sodium titanate type $Na_2Ti_3O_7$ was not identified under the characteristic maximum intensity diffraction peak at 2θ of 9.68°, which did not appear next to characteristic peaks of $Na_2Ti_6O_{13}$ [22]. For the rest of 2θ values of $Na_2Ti_3O_7$ at 24.35°, 28.20°, 48.20°, and 60.86°, all those could have superposed with the pattern of $Na_2Ti_6O_{13}$. Also, TiO_2 crystalline secondary phase presence was not identified, because the maximum intensity peak of the diffraction angle characteristic to this phase at 2θ= 25.1° (101) could not have been observed on the plot, leading to the conclusion that the entire quantity of $TiCl_4$ was used for the two titanates [23]. The crystallite size of the plane with Miller indices (200) of sodium titanate $Na_2Ti_6O_{13}$ was calculated at ~22 nm using from the width of diffraction peaks using the Scherrer equation (1):

$$D=(0.9\lambda)/\beta\cos\theta \quad (1)$$

where λ is Xray wavelength of 1.54056 Å, β is full width half maxima, θ is Bregg's diffraction angle.

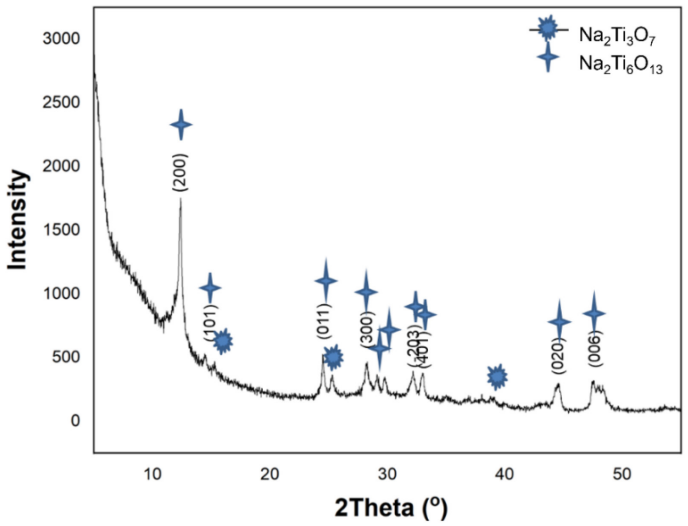

Fig. 1. XRD pattern of the synthesized sodium titanate powder

3.2 Thermogravimetry measurements

The sodium titanate powder was analysed at the Thermogravimetric analyser, before its annealing at 600°C for 2 h in air atmosphere (Fig. 2). Between 100 and 200°C, the sodium titanate obtained by sol-gel has lost 17.87 wt% of water as could it be seen in Fig. 2, on the TG curve. The low temperature of the water released indicates that it appeared in a physiosorbed state in the titanate powder. Hence, for the as-prepared sodium titanate, the water content decreased by more than 5 wt.%, this means that some water contamination still occurred in the titanate powder, taking into consideration the hydrophilic nature of this material. The occurrence of water contamination in the obtained sodium titanate shows their capability to easily adsorb water from the environment. In addition, the TG broad line remained almost unchanged after 300°C (Figure 2). This evidenced a preservation of the crystal structure of the sodium titanate during the release of physiosorbed water. At a close

examination of the DTA curve, the profile revealed a high-intensive peak at around 400°C showing an exotherm process, which can be attributed to structural water loss, that is stronger bonded at the crystalline structures than adsorbed one, and a higher energy it is consumed for its removal. The shoulder of DTA curve at around 800°C, marked another exothermic effect that could be assigned to polymorphic transformation of titanates [24].

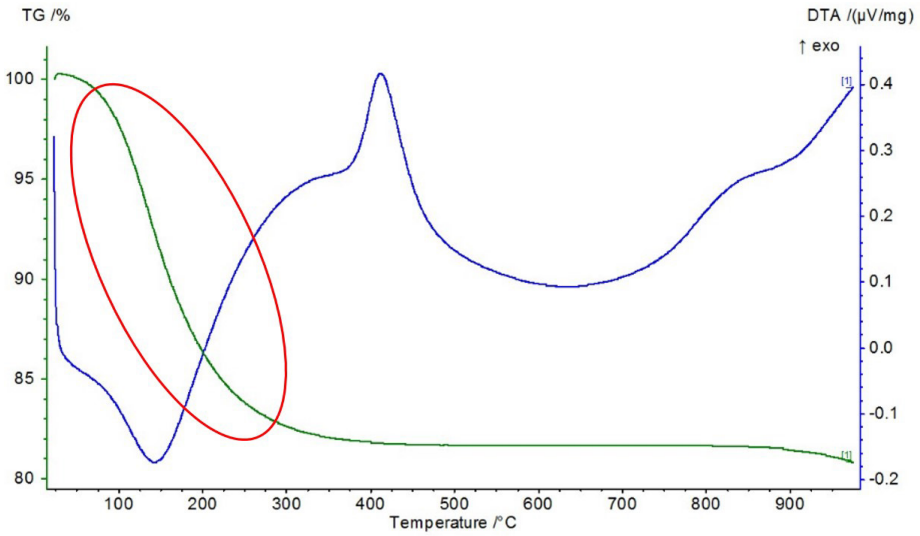

Fig. 2. TG and DTA curves of sodium titanates synthetized by sol-gel method and hydrothermal maturation

3.3 Texture and morphostructure characterization of sodium titanate

The electron microscopy (SEM) and energy dispersive spectroscopy (EDS) analyses provided further information on the morphology and structure of the sol-gel synthesis and hydrothermally maturated sodium titanate powder, with its two phases $Na_2Ti_3O_7$ and $Na_2Ti_6O_{13}$. The SEM images at increasing magnifications and on different section scanned, have shown that the texture of sample consist of a mixture of sodium titanate particles in the form of wires and platelets, probably the crystals having different morphology considering the different Ti content of the two phases (n= 3 and 6), grown as a result of the calcination treatment (Fig. 3 a-d). By increasing the magnification (Fig. 3 c and d), it can be noticed that the wires and platelets tend to stick one another, thus forming a bundle of structures distributed and oriented in various directions. It is worth mentioning that the morphology of $Na_2Ti_3O_7$ prepared by the sol-gel reaction and hydrothermal maturation, consisted of wires as reported before [21]. The mean dimensions of wires like particles are: length of 3.1549 ± 1.0181µm and the mean diameter of 0.4224 ± 0.2267µm, while the limits of platelet like particles were unable to be measured considering their agglomeration and overlapping. Obviously, the wires of $Na_2Ti_3O_7$ tend to develop on the base platelets of $Na_2Ti_6O_{13}$, which represent the major crystalline phase of the powder.

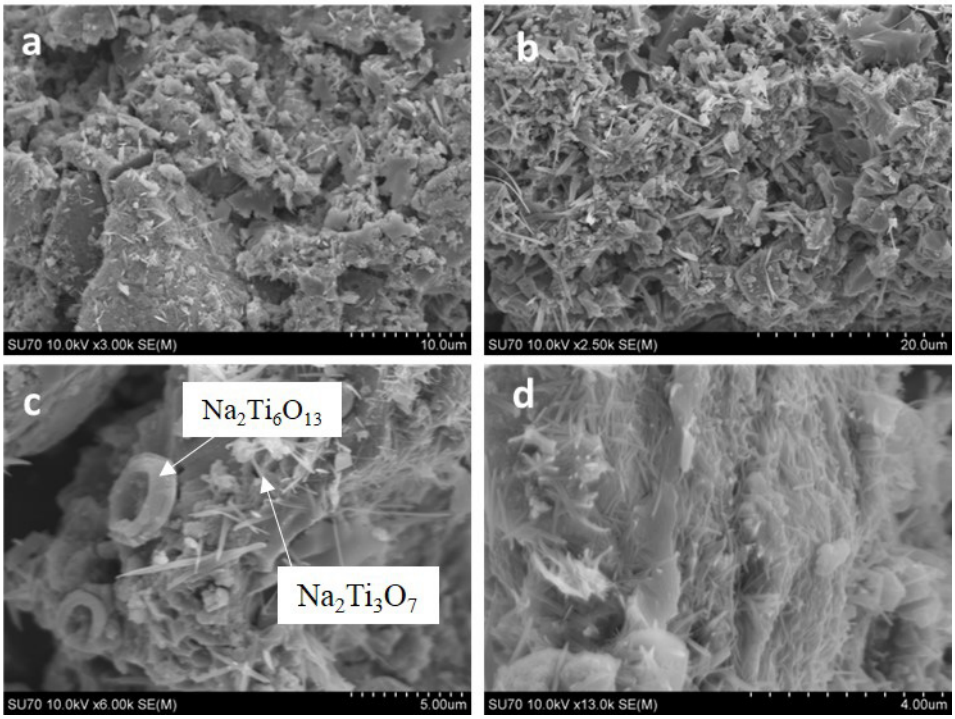

Fig. 3. SEM micrographs of the sodium titanate powder hydrothermally and calcination treated at magnification (a) 3000x, (b) 2500x, (c) 6000x, (d)13,000x

Energy dispersive spectroscopy (EDS) was used to confirm the existence of Na in the hydrothermally treated samples. Fig.4 (a) shows the distribution mapping of Na and Ti elements contained in the section of the analysed sodium titanate powder. The homogenic distribution of the two elements can be observed. EDS spectrum of the sample identifies also C, O, Na, Ti and Au, the latter from the thin Au-Pd coating used to improve the electrical conductivity of the samples (Fig. 4 (b)).

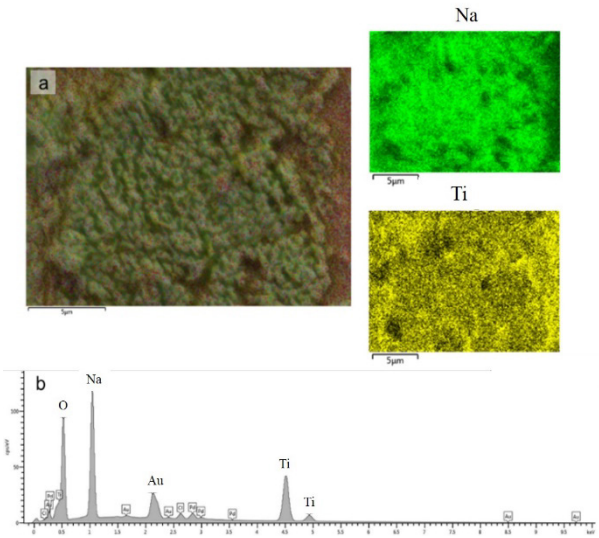

Fig. 4. a) EDS elemental map and b) EDS spectrum of the obtained sodium titanate particles

4 Conclusions

An unconventional synthesis method for sodium titanate was approached, starting from $TiCl_4$ and NaOH precursors. The regents were left to react in cold conditions, then after the formation of the precipitate, it was separated and matured hydrothermally. Finally, for a high degree of crystallinity, a thermal treatment was applied at high temperatures, for a short period of time. Compositionally characterized by XRD, the powder showed the coexistence of two crystalline phases of sodium titanates $Na_2Ti_3O_7$ and $Na_2Ti_6O_{13}$, and the absence of the crystalline phase of TiO_2, which meant that they were formed directly, without the intermediate formation of TiO_2. During the SEM analysis, it was observed that the two phases of sodium titanate have different morphologies: wires and platelets. The study demonstrated that the unconventional method in a single step can generate sodium titanate powders that can be used to obtain ceramics used in numerous applications such as photocatalysis, sodium batteries, or the realization of sensors and wastewater purification.

Acknowledgement

This work was carried out through project Institutional development of the National Institute for Research and Development in Environmental Protection Bucharest in order to increase the capacity and performance in the field of environmental protection and climate change (2022-2024) - No.39PFE/30.12.2021.

References

1. A.K.G. Oliveira, A.P.B. Santos, V.P.d.S. Caldeira, Per. Tchê Quim. **17** 436-447 (2020)
2. M.D. Wadge, Developing Unique Nanoporous Titanate Structures for Biomedical Applications: Mechanisms, Conversion and Substitution, University of Nottingham (2020)
3. M.D. Wadge, J. McGuire, K.G. Thomas, B.W. Stuart, R.M. Felfel, I. Ahmed, D.M. Grant, Int. Mater. Rev. **68** 677-724 (2023)
4. Q.Z. Cheng-Yan Xu, H. Zhang, L. Zhen, J. Tang, L. Chang, J. Am. Chem. Soc. 11584-11585 (2005)
5. M. Kim, G. Choi, D. Yoo, K. Lee, MRS Proceedings **1784** (2015).
6. F. Marinescu, M.C. Chifiriuc, L. Marutescu, M. Ilie, I. Savin, A.M. Anghel, I. Marcus, C. Tociu, E. Marcu, Biointerface Res. Appl. Chem. **7** 2140-2144 (2017)
7. Gy. Deák, F.D. Dumitru, M.A. Moncea, A.M. Panait, M. Boboc, T. Dănălache, E. Holban, F. Marinescu, P.I. Gheorghe, I. Ciobotaru, M.R. Rozainy, AIP Conf. Proc. **2129** 1 (2019)
8. Y. Kondo, T. Goto, T. Sekino, RSC Adv **10** 41032-41040 (2020)
9. Gy. Deak, V. Daescu, E. Holban, P. Marinescu, G.S. Tanase, R. Csergo, A.I. Daescu, S. Gaman, J. Environ. Prot. Ecol. **16** 304-315 (2015)
10. M. Tayebi, Z. Masoumi, B.K. Lee, Ultrason Sonochem, **70** 105339 (2021)
11. A.H. Zaki, A.A. Naeim, S.I. El-Dek, Environ Sci Pollut Res Int, **26** 36388-36400 (2019)
12. G. Kim, D.S. Lee, H. Eccles, S.M. Kim, H.U. Cho, J.M. Park, RSC Adv, **12** 18936-18944 (2022)
13. P. Umek, A. Gloter, C. Navio, C. Bittencourt, AIP Conf. Proc. **1415** 24–27 (2011)

14. M. Zhao, S. Wang, H. Wang, P. Qin, D. Yang, Y. Sun, F. Kong, Environ. Pollut. **248** 938-946 (2019)
15. A.H. Zaki, S. Adel, M.M. Abd El-Hafiez, A.A. Abdel-Khalek, Beni-Suef University Journal of Basic and Applied Sciences **10** (2021)
16. Z. Noer, T. Sembiring, K. Sebayang, M.N. Nasruddin, R. Septawendar, B. Sunendar, AIP Conf. Proc. **2221** 110027 (2020)
17. O. Cech, K. Castkova, L. Chladil, P. Dohnal, P. Cudek, J. Libich, P. Vanysek, J. Energy Storage **14** 391-398 (2017)
18. J.A. Knoll, N. Pennisi, P.A. Yarnell, Patent no. US20120103911A1 (2010)
19. Y. Zhang, G. Li, J. Liu, T. Wang, X. Wang, B. Liu, Y. Liu, Q. Huo, Z. Chu, J. Colloid. Interface Sci. **528** 109-115 (2018)
20. A.L. Sauvet, S. Baliteau, C. Lopez, P. Fabry, J. Solid State Chem. **177** 4508–4515 (2004)
21. M.N. Akieh, M. Lahtinen, A. Vaisanen, M. Sillanpaa, J. Hazard. Mater. **152** 640-647 (2008)
22. J. Wang, J. Bi, W. Wang, Z. Xing, Y. Bai, M. Leng, X. Gao, J. Electrochem. Soc. **167** (2020)
23. C.H. Lee, S.W. Rhee, H.W. Choi, Nanoscale Res. Lett. **7** 48 (2012)
24. R.A. Zárate, S. Fuentes, J.P. Wiff, V.M. Fuenzalida, A.L. Cabrera, J. Phys. Chem. **68** 628-637 (2007)